CHAPTER IV
RESULTS AND DISCUSSION

4.1 Gas Chromatography Analysis

Analysis of the compounds in the feed and product mixture was done by gas chromatography. The instrument model which is used for analysis is the Hewlett Packard HP 5890 Series II GC system equipped with a flame ionizing detector. The concept behind the instrument is the separation of gaseous mixture compounds due to its vapor pressure property.

Pre-analysis needs to be done in order to obtain the retention time and response factor, which will be used for calculation in further analysis.

A mixture of the standard was prepared. The standards were selected by using the typical components found in the epoxidation of cyclohexene, which includes cyclohexene, cyclohexene oxide, 2-cyclohexen-1-ol, 2-cyclohexen-1-one and (1S,2S)-tran-1,2-cyclohexanediol. Dodecane was used as the internal standard. Approximately 0.3 g of each standard was added into 1 ml of the solvent, tert-butanol. The standard mixture was injected into the GC-FID with the same conditions which would be used for analysis of the products shown in Table 4.1.

Table 4.1 GC conditions for product analysis

Setting	Condition
Oven temperature	50 °C for 5 min, 10 °C/min to 160 °C, 160 °C for 5 min
Injector temperature	250°C
Detector temperature	250°C
Carrier gas	Helium 99.99 %purity
Sample volume	1 μl
Column type	ZB-5 HT column (30 m × 0.32 mm ID × 0.10 μm Film Thickness)

The retention time of each component was found on the x-axis of the chromatogram. The response factor was calculated from the equation 4.1 and summarized in Table 4.2.

$$R_x = \left(\frac{m_{is}}{A_{is}}\right)\left(\frac{A_x}{m_x}\right)$$
(4.1)

Table 4.2 Retention time and response factor of each substance from GC analysis

| Number	Substance	Retention time (min)	Response factor
1	*tert*-Butanol (solvent)	4.08	-
2	cyclohexene	4.57	0..81
3	cyclohexene oxide	6.66	0.86
4	2-cyclohexen-1-ol	7.42	1.07
5	2-cyclohexen-1-one	8.40	0.91
6	*trans*-1,2-cyclohexanediol	11.48	0.61
7	dodecane	14.00	1.03

Analysis of the catalytic activity was done over a variety of parameters. Apart from the basis catalysts (sol-gel TiO_2, 1%Ru/TiO_2, and 2%Ce/TiO_2) and variation of Ce loading, the parameters studied are divided into two groups, calcination and reaction parameters.

4.1.1 GC results of sol-gel TiO_2, 1%Ru/TiO_2, and 2%Ce/TiO_2

The first experiments were to identify the productivity of the basis catalysts. The catalysts include sol-gel TiO_2, 1%Ru/TiO_2, and 2%Ce/TiO_2. They would be used as the basis for comparison of the Ce/Ru/TiO_2 catalysts studied in this thesis. Figures 4.1 – 4.3 depict the conversion, selectivity and yield of the catalysts. The three catalysts were all active for cyclohexene epoxidation. Sol-gel TiO_2 (12.0 %conversion; 15.7 %cyclohexene oxide selectivity; 1.9 %yield) gave the lowest productivity while 2%Ce/TiO_2 gave the highest (19.6 %conversion; 49.5

%cyclohexene oxide selectivity; 9.7 %yield). Addition of metal into the TiO_2, forming bimetallic catalyst, helps aid the cyclohexene epoxidation reaction.

The sol-gel TiO_2 was more selective towards the by-products, especially *trans*-1,2-cyclohexanediol, which is likely to be produced by ring-opening of the epoxide. The proposed mechanism is shown in Figure 4.25 (N. Bao *et al.*, 2010) and Figure 4.26 (A.S. Reddy *et al.*, 2010). According to the mechanism, even though the epoxides are formed, they continue to react, forming the by-product. The 1%Ru/TiO_2 catalyst shows better selectivity towards cyclohexene oxide than the typical sol-gel TiO_2. The 2%Ce/TiO_2 shows exceptional results for production of cyclohexene oxide but tends to also effectively discourage further ring-opening reactions. The higher selectivity towards cyclohexene oxide responds to the surface area results shown in Table 4.3. The bimetallics have higher surface area and porous volume. The higher amount of accessibility towards the active sites enhances the occurrence of the reaction, increasing the conversion and selectivity.
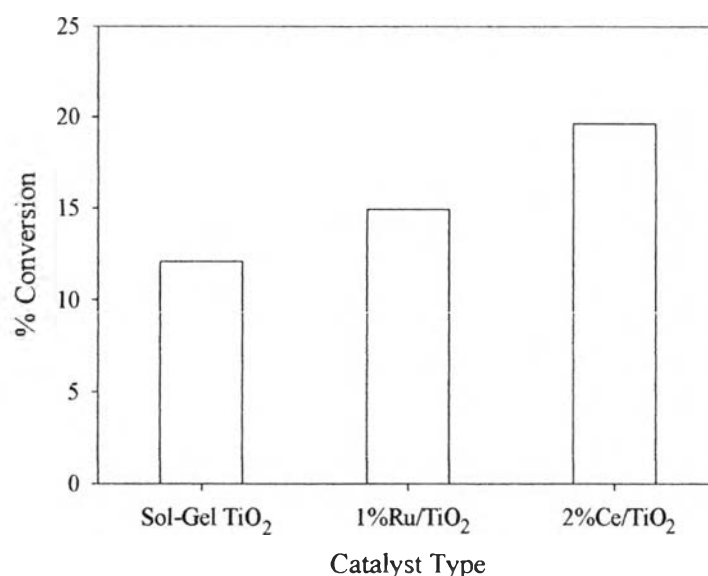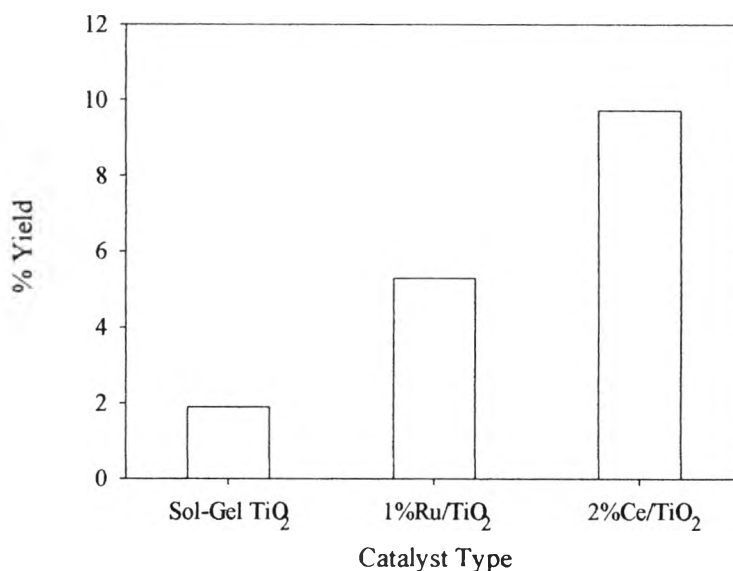

Figure 4.1 Conversion of sol-gel TiO_2, 1%Ru/TiO_2, and 2%Ce/TiO_2.

(Reaction conditions: calcined at 500 °C for 4 hours, 0.5 g of catalyst, 30 mmol of cyclohexene, 30 mmol of hydrogen peroxide and 70 °C reaction temperature)
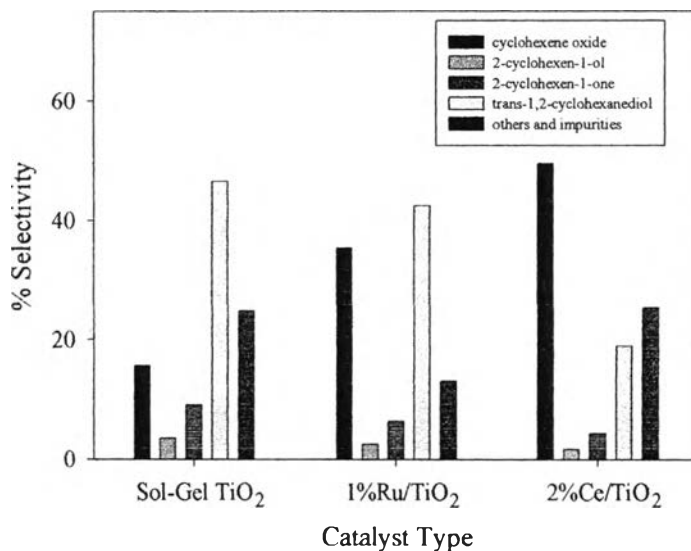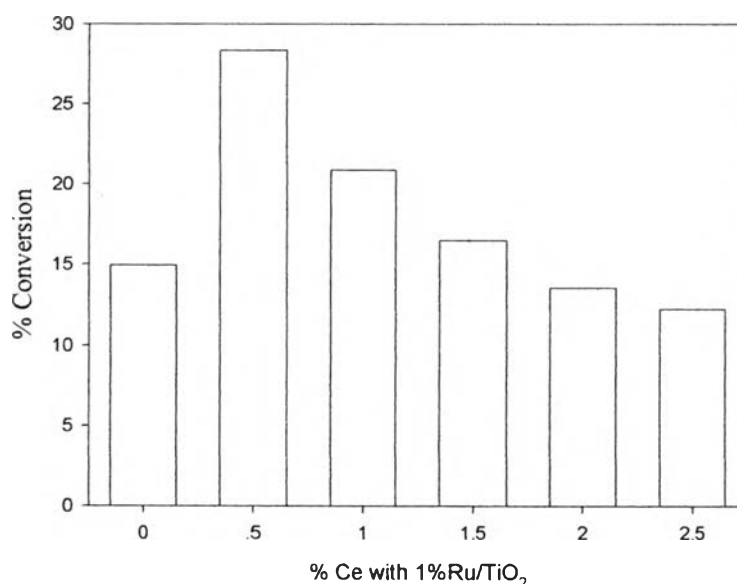
Figure 4.2 Selectivity of sol-gel TiO_2, 1%Ru/TiO_2, and 2%Ce/TiO_2.

(Reaction conditions: calcined at 500 °C for 4 hours, 0.5 g of catalyst, 30 mmol of cyclohexene, 30 mmol of hydrogen peroxide and 70 °C reaction temperature)

Figure 4.3 Yield of sol-gel TiO_2, 1%Ru/TiO_2, and 2%Ce/TiO_2.

(Reaction conditions: calcined at 500 °C for 4 hours, 0.5 g of catalyst, 30 mmol of cyclohexene, 30 mmol of hydrogen peroxide and 70 °C reaction temperature)

4.1.2 Effect of Ce Loading on 1%Ru/TiO₂

The variation on Ce loading onto the 1%Ru/TiO₂ support was investigated. The Ce loading was varied between 0.5, 1.0, 1.5, 2.0, 2.5 and 3.0 % on 1%Ru/TiO₂ support. The increase of the Ce metal loading has high conversion at lower loadings which is shown in Figure 4.4. 0.5%Ce/1%Ru/TiO₂ had the highest conversion (28.3 %conversion). In terms of cyclohexene oxide selectivity, Figure 4.5, the selectivity is not affected by the variation of Ce loading. The results are averagely 64.5 % with a ±1% fluctuation. The productivity of the catalyst is decided by the yield which was highest (17.9) with 0.5%Ce/1%Ru/TiO₂.
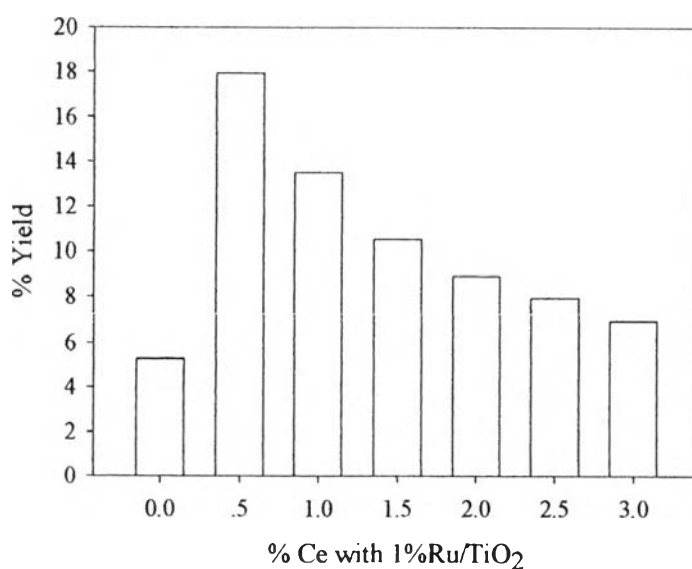

Figure 4.4 Conversion of Ce content variation with 1%Ru/TiO₂.

(Reaction conditions: calcined at 500 °C for 4 hours, 0.5 g of catalyst, 30 mmol of cyclohexene, 30 mmol of hydrogen peroxide and 70 °C reaction temperature)
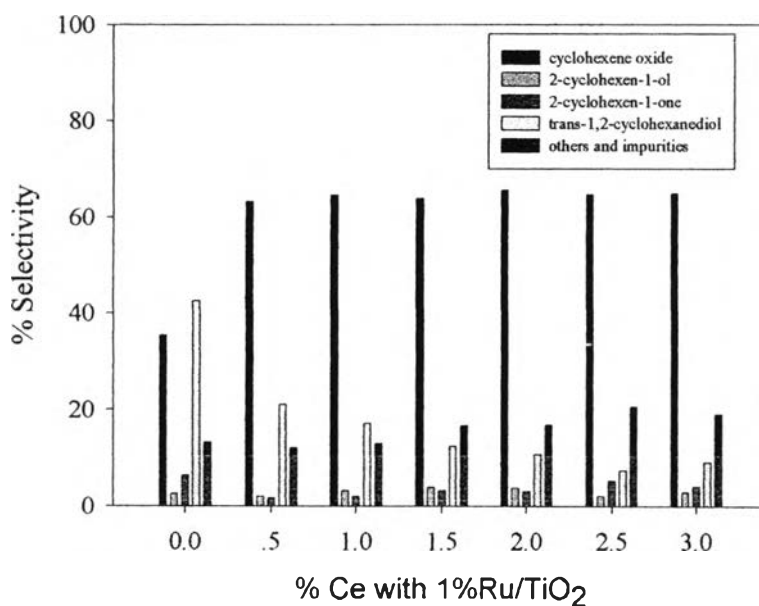
Figure 4.5 Selectivity of Ce content variation with 1%Ru/TiO₂.

(Reaction conditions: calcined at 500 °C for 4 hours, 0.5 g of catalyst, 30 mmol of cyclohexene, 30 mmol of hydrogen peroxide and 70 °C reaction temperature)
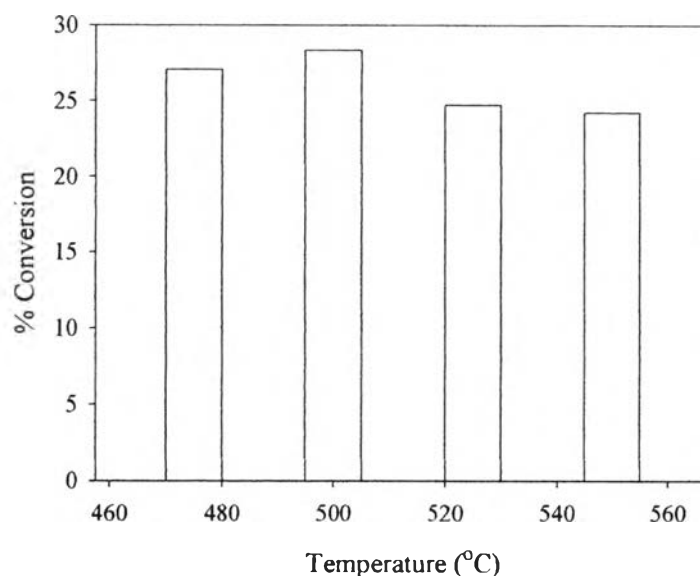

Figure 4.6 Yield of Ce content variation with 1%Ru/TiO₂.

(Reaction conditions: calcined at 500 °C for 4 hours, 0.5 g of catalyst, 30 mmol of cyclohexene, 30 mmol of hydrogen peroxide and 70 °C reaction temperature)

The tri-metallic catalyst better promotes cyclohexene epoxidation when compared with the bi-metallic ($1\%Ru/TiO_2$) catalyst. The amount of metal loaded on the TiO_2 support is consistent with the density of surface hydroxyls found on the catalyst. In other words, the $Ce/Ru/TiO_2$ catalyst has higher surface hydroxyls than the bi-metallic ($1\%Ru/TiO_2$) catalyst. It can be inferred that the surface hydroxyls are directly affecting the performance of the reaction. The higher addition of Ce inhibits the surface OH structure; therefore, Ce may be discouraging dispersion of the active sites on the catalysts.

### 4.1.3 Effect of Calcination Parameters

Calcination parameters that were studied are calcination temperature, calcination time, and calcination ramp rate. The calcination temperature gave the optimum yield at 500 °C. The productivity was best when calcined for 4 hours at a ramp rate of 1°C/min. The effect of calcination parameters are depicted in Figure 4.7 – 4.15.

Figure 4.7 Conversion of $0.5\%Ce/1\%Ru/TiO_2$ with varying calcination temperature. (Reaction conditions: calcined for 4 hours, 0.5 g of catalyst, 30 mmol of cyclohexene, 30 mmol of hydrogen peroxide and 70 °C reaction temperature)
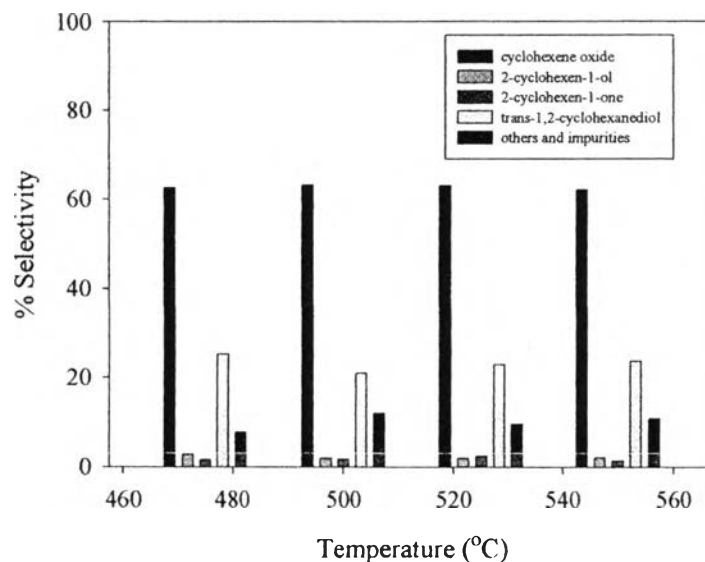
Figure 4.8 Selectivity of 0.5%Ce/1%Ru/TiO$_2$ with varying calcination temperature. (Reaction conditions: calcined for 4 hours, 0.5 g of catalyst, 30 mmol of cyclohexene, 30 mmol of hydrogen peroxide and 70 °C reaction temperature)
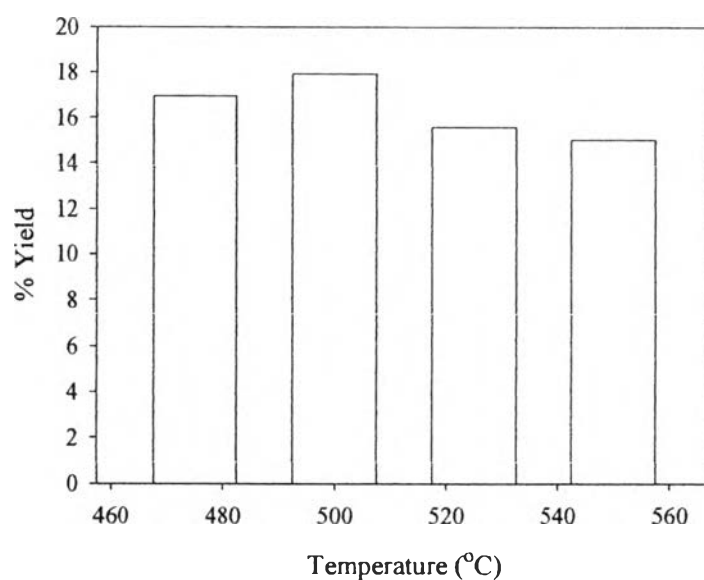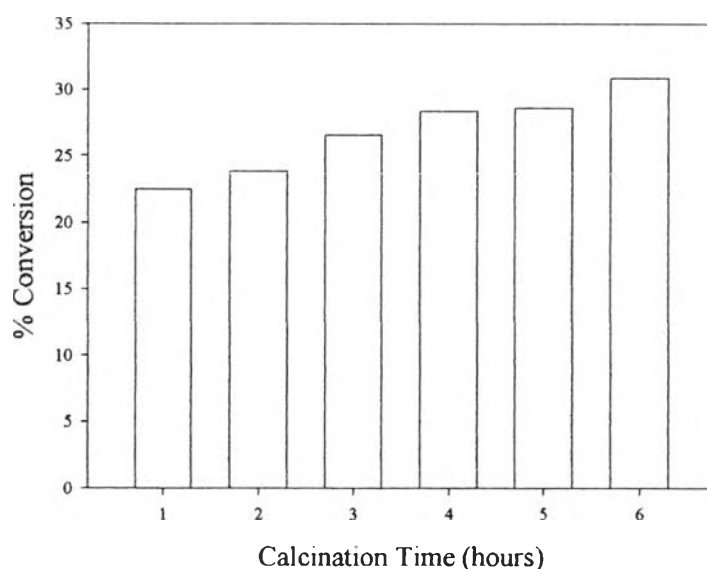

Figure 4.9 Yield of 0.5%Ce/1%Ru/TiO$_2$ with varying calcination temperature. (Reaction conditions: calcined for 4 hours, 0.5 g of catalyst, 30 mmol of cyclohexene, 30 mmol of hydrogen peroxide and 70 °C reaction temperature)
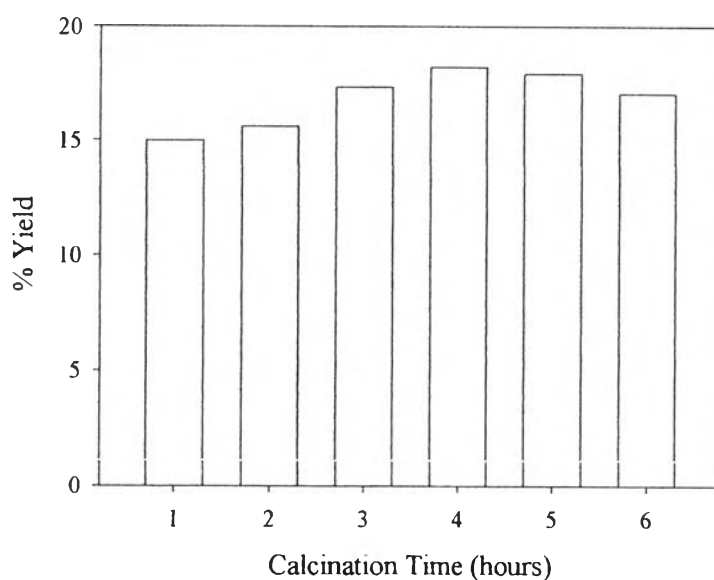
The calcination temperature was varied between 475-550 °C. A temperature of 500°C for calcination should be sufficient enough to remove all unwanted components in the catalyst during calcination as well as being above the temperature the catalyst undergoes the phase changes. The 450°C temperature for calcination gave a slightly lower conversion and selectivity, as the catalyst is not yet fully crystallized. In addition, even though the catalyst had a higher surface area, a more important factor was the density of the surface hydroxyl which was 3.148 /nm^2 for the calcination temperature 0f 475°C while calcination at 500 °C achieved 3.164 /nm^2. The less surface hydroxyl leads to less probability towards the reaction pathway. Calcination temperatures above 500 °C show a decrease in surface hydroxyl. The surface area is clearly decreased with larger pore diameter, indicating collapsing of the porous structure. In addition, previous researches by Woragamon et al. in 2010 shows that calcination at higher temperatures (600-700 °C) causes the catalyst to undergo phase crystallization again.

Figure 4.10 Conversion of 0.5%Ce/1%Ru/TiO$_2$ with various calcination times. (Reaction conditions: calcined at 500 °C, 0.5 g of catalyst, 30 mmol of cyclohexene, 30 mmol of hydrogen peroxide and 70 °C reaction temperature)
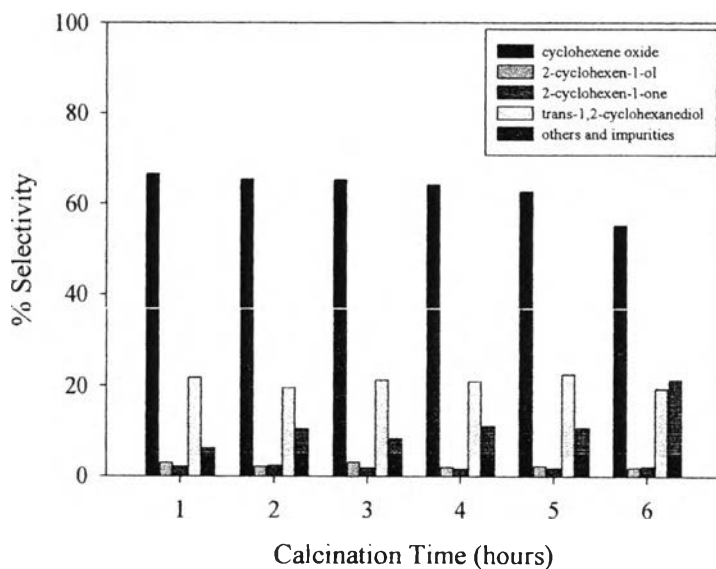
Figure 4.11 Selectivity of 0.5%Ce/1%Ru/TiO$_2$ with various calcination times. (Reaction conditions: calcined at 500 °C, 0.5 g of catalyst, 30 mmol of cyclohexene, 30 mmol of hydrogen peroxide and 70 °C reaction temperature)

Figure 4.12 Yield of 0.5%Ce/1%Ru/TiO$_2$ with various calcination times. (Reaction conditions: calcined at 500 °C, 0.5 g of catalyst, 30 mmol of cyclohexene, 30 mmol of hydrogen peroxide and 70 °C reaction temperature)

The calcination time was studied over the range of 1-6 hours. The calcination time increases the conversion. However, at longer calcination times, the selectivity of cyclohexene decreases while the minor by-products and impurities increase significantly. The optimum time is therefore selected by comparison of the yield, which 4 hours gave the highest yield at 18.2%. At calcination times lower than 4 hours, the catalyst has lower surface hydroxyl densities although the surface area is higher. This indicates that the surface hydroxyl in this parameter is more dependent on the weight loss from the TG/DTA. At longer times, the surfactant templating reagent as well as other solvents and organic remnants are removed. The removal of all unwanted components along with crystallization transitions are done at 4 hours, the optimum time. After 4 hours, longer exposure to the heat causes the diameter of the pores to significantly increase, lowering the surface area, which in turn, lowers the surface hydroxyl sites.
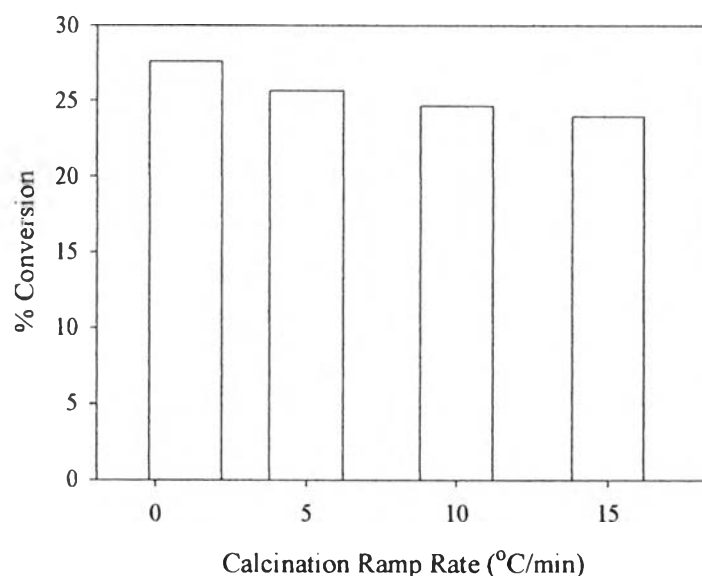
Figure 4.13 Conversion of 0.5%Ce/1%Ru/TiO$_2$ with various calcination ramp rates. (Reaction conditions: calcined at 500 °C for 4 hours, 0.5 g of catalyst, 30 mmol of cyclohexene, 30 mmol of hydrogen peroxide and 70 °C reaction temperature)
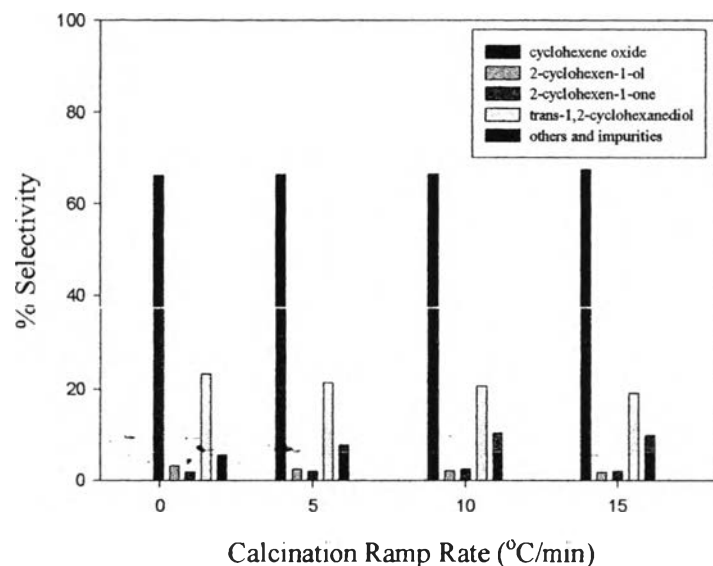
Figure 4.14 Selectivity of 0.5%Ce/1%Ru/TiO₂ with various calcination ramp rates. (Reaction conditions: calcined at 500 °C for 4 hours, 0.5 g of catalyst, 30 mmol of cyclohexene, 30 mmol of hydrogen peroxide and 70 °C reaction temperature)
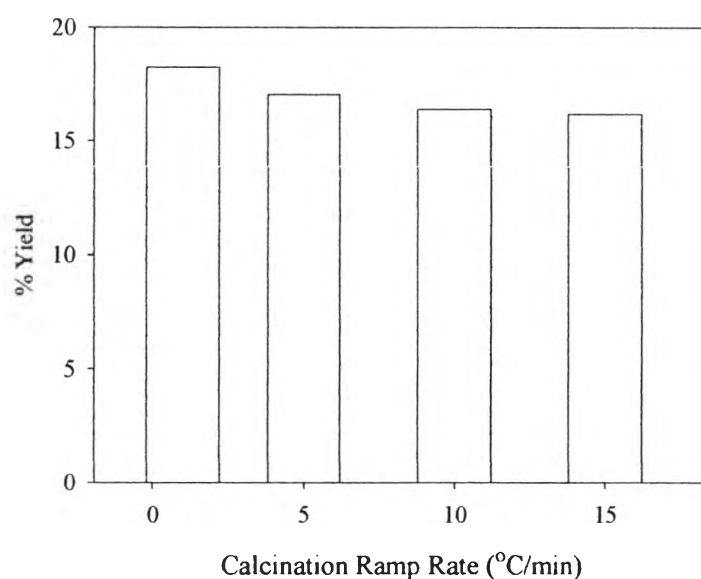
Figure 4.15 Yield of 0.5%Ce/1%Ru/TiO₂ with various calcination ramp rates. (Reaction conditions: calcined at 500 °C for 4 hours, 0.5 g of catalyst, 30 mmol of cyclohexene, 30 mmol of hydrogen peroxide and 70 °C reaction temperature)

The calcination ramp rate is studied by varying; 1 °C/min, 5 °C/min, 10 1°C/min, and 15 1°C/min. Lower calcination ramp rates encourages the catalyst's performance. Rapid increase in the calcination temperature may cause destruction of the porous structures, causing lower surface areas, which lowers the surface hydroxyls.

4.1.4 Effect of Reaction Parameters

Reaction parameters that were taken into consideration include the catalyst amount, reaction temperature, reaction time and C_6H_6-to-H_2O_2 ratio. The catalyst was most efficient at 70 °C, working with a C_6H_6-to-H_2O_2 ratio of 1 and using 50 mg of the catalyst.
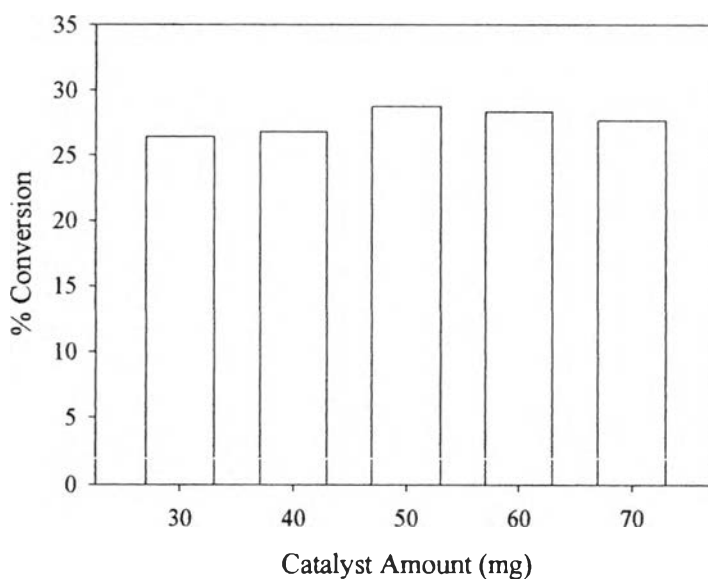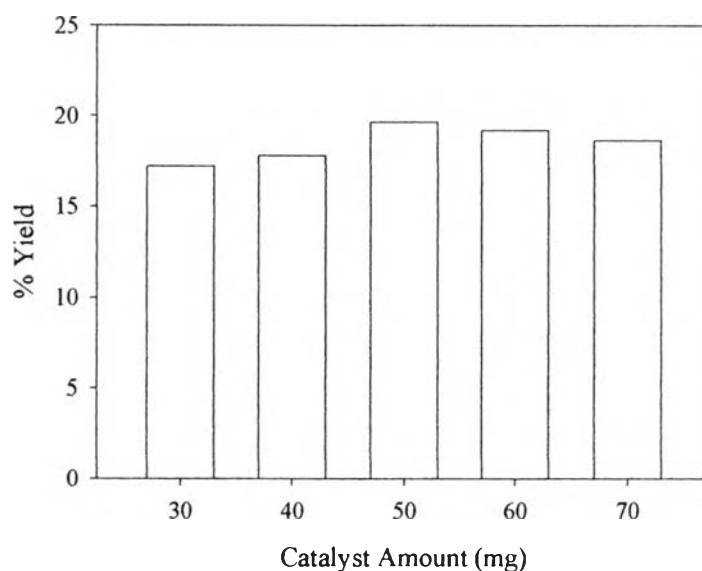

Figure 4.16 Conversion of 0.5%Ce/1%Ru/TiO$_2$ with various catalyst amounts. (Reaction conditions: calcined at 500 °C for 4 hours, 30 mmol of cyclohexene, 30 mmol of hydrogen peroxide and 70 °C reaction temperature)
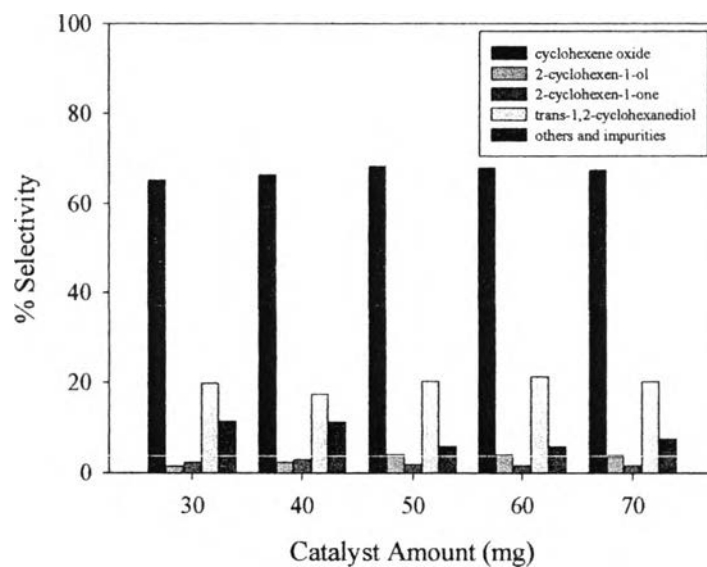
Figure 4.17 Selectivity of 0.5%Ce/1%Ru/TiO$_2$ with various catalyst amounts. (Reaction conditions: calcined at 500 °C for 4 hours, 0.5 g of catalyst, 30 mmol of cyclohexene, 30 mmol of hydrogen peroxide and 70 °C reaction temperature)

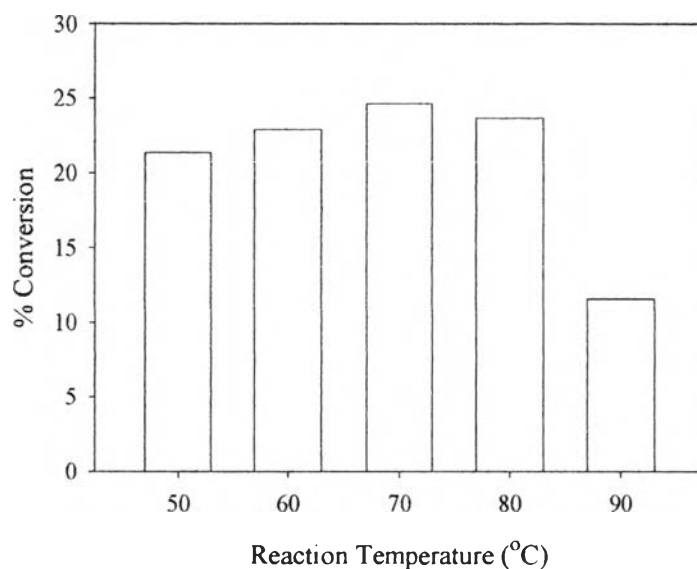**Figure 4.18** Yield of 0.5%Ce/1%Ru/TiO$_2$ with various catalyst amounts. (Reaction conditions: calcined at 500 °C for 4 hours, 0.5 g of catalyst, 30 mmol of cyclohexene, 30 mmol of hydrogen peroxide and 70 °C reaction temperature)

Figure 4.19 Conversion of 0.5%Ce/1%Ru/TiO₂ at various reaction temperatures. (Reaction conditions: calcined at 500 °C for 4 hours, 0.5 g of catalyst, 30 mmol of cyclohexene, and 30 mmol of hydrogen peroxide)
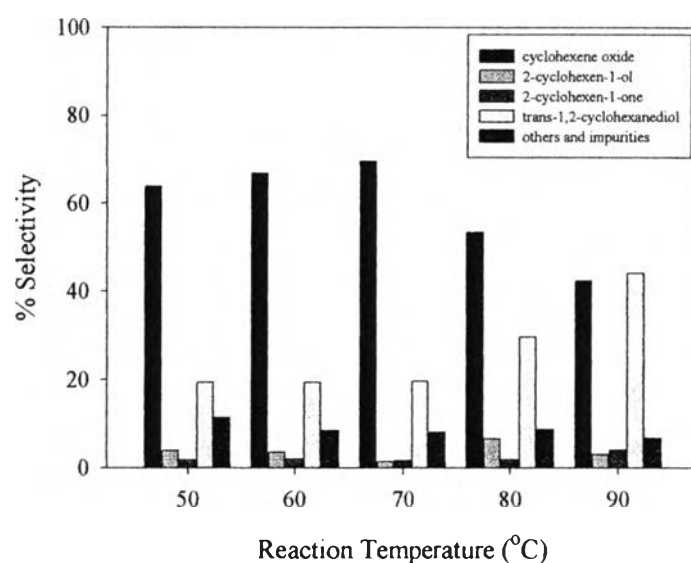

Figure 4.20 Selectivity of 0.5%Ce/1%Ru/TiO₂ with various catalyst amounts. (Reaction conditions: calcined at 500 °C for 4 hours, 0.5 g of catalyst, 30 mmol of cyclohexene, and 30 mmol of hydrogen peroxide)
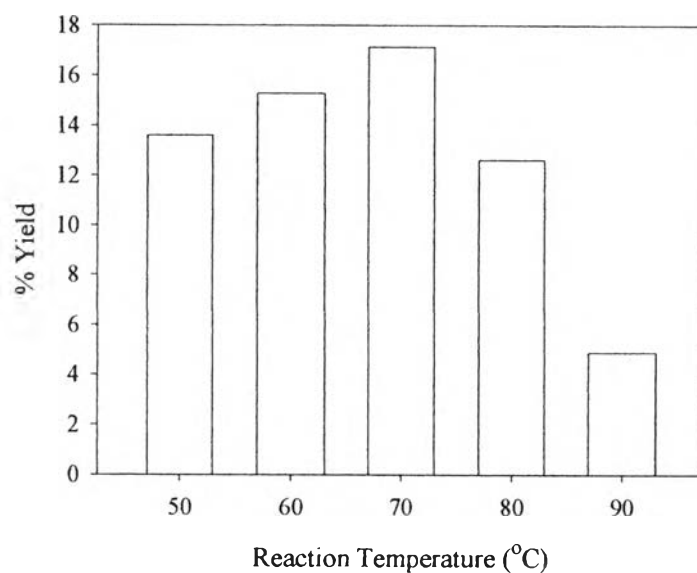
Figure 4.21 Yield of 0.5%Ce/1%Ru/TiO$_2$ with various catalyst amounts.
(Reaction conditions: calcined at 500 °C for 4 hours, 0.5 g of catalyst, 30 mmol of cyclohexene, and 30 mmol of hydrogen peroxide)

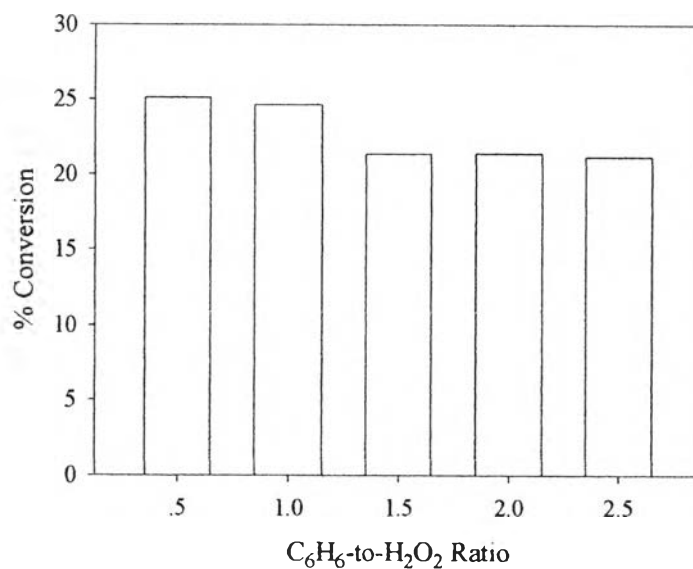**Figure 4.22** Selectivity of 0.5%Ce/1%Ru/TiO$_2$ with various C$_6$H$_6$-to-H$_2$O$_2$ ratios.
(Reaction conditions: calcined at 500 °C for 4 hours, 0.5 g of catalyst and 70 °C reaction temperature)
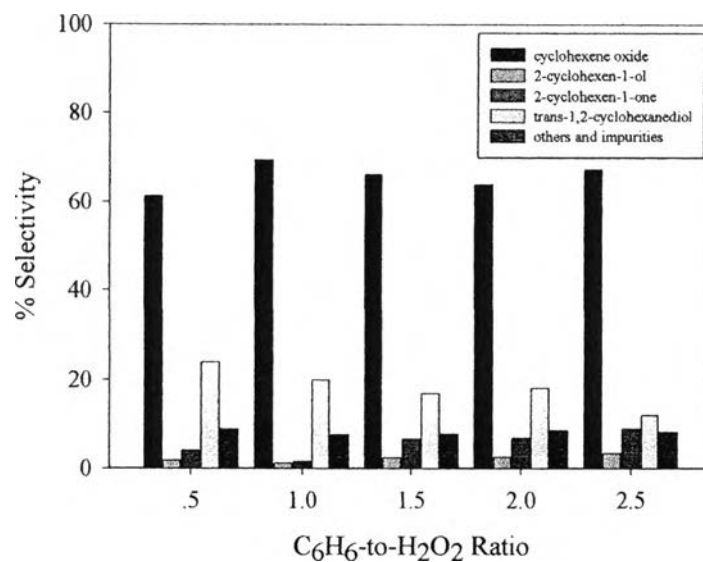
Figure 4.23 Selectivity of 0.5%Ce/1%Ru/TiO$_2$ with various C$_6$H$_6$-to-H$_2$O$_2$ ratios. (Reaction conditions: calcined at 500 °C for 4 hours, 0.5 g of catalyst and 70 °C reaction temperature)

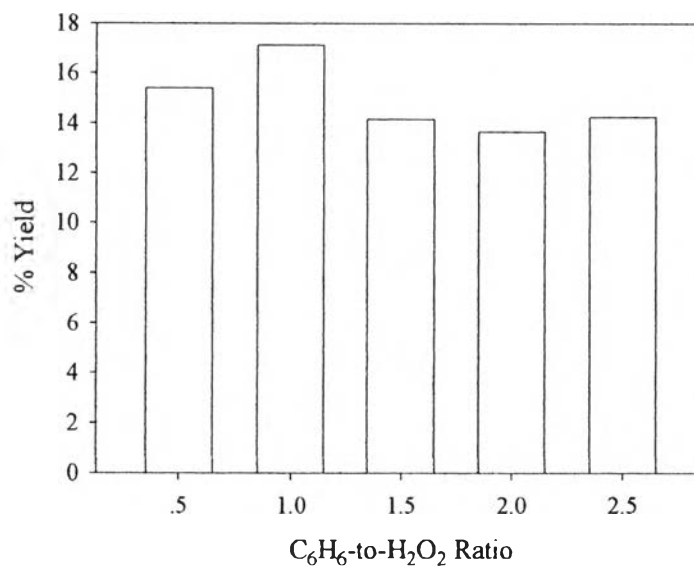**Figure 4.24** Selectivity of 0.5%Ce/1%Ru/TiO$_2$ with various C$_6$H$_6$-to-H$_2$O$_2$ ratios. (Reaction conditions: calcined at 500 °C for 4 hours, 0.5 g of catalyst and 70 °C reaction temperature)
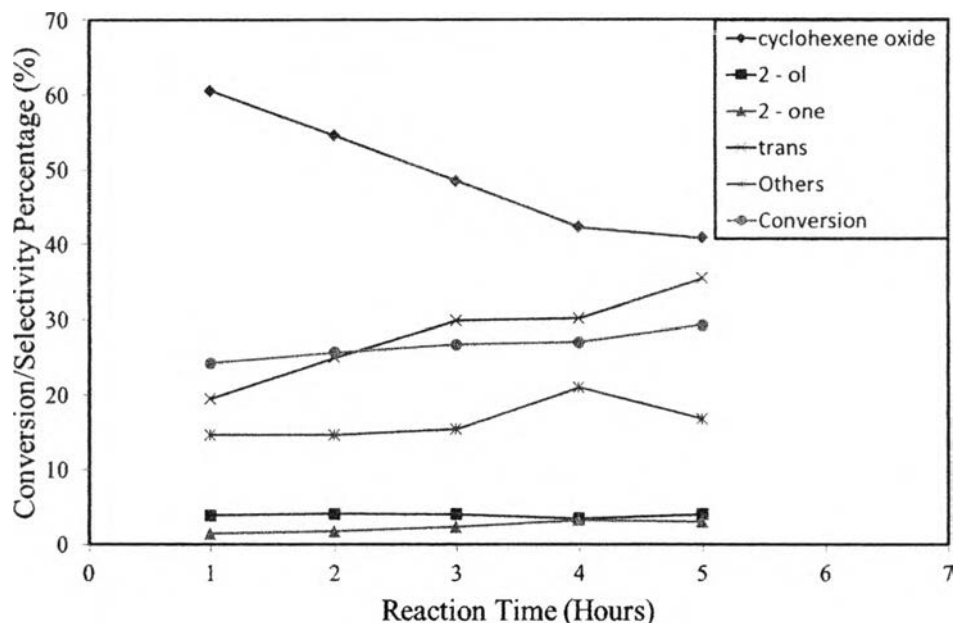
Figure 4.25 Conversion and Selectivity of 0.5%Ce/1%Ru/TiO$_2$ with various reaction times. (Reaction conditions: calcined at 500 °C for 4 hours, 0.5 g of catalyst and 70 °C reaction temperature)

Due to pre-experiments, the hydrogen peroxide-to-cyclohexene ratios were investigated in the earlier stages of the research since they have shown to be highly effective towards the product selectivity. The cyclohexene epoxidation experiment was tested using ratios of 0.5, 1, 1.5, 1, and 2.5 by fixing the amount of cyclohexene. The conversion, selectivity and yield were examined using the GC-FID represented by Figures 4.22 – 4.24.

The reaction time was investigated for 5 hours. Conversion steadily increases with time. However, the increase is not due to cyclohexene, but due to a faster increase of *trans*-1,2-cyclohexanediol.

The optimum ratio is 1 (24.6 %conversion; 69.6 %cyclohexene oxide selectivity; 17.1 %yield). Below the ratio of 1, there seems to be insufficient hydrogen peroxide for a complete cyclohexene epoxidation. However, after the ratio of 1, the abundant amount of hydrogen peroxide shows that the conversion is steady while the selectivity towards cyclohexene oxide decreases. This implies that the side

reaction, especially for the conversion of 2-cyclohexen-1-one and (1S,2S)-tran-1,2-cyclohexanediol, is replacing the conversion towards cyclohexene oxide.

The common side reactions are from allylic oxidation and ring-opening of the epoxide. Ring-opening of the epoxide gives the diol as the by-product while allylic oxidation causes 2-cyclohexen-1-one and 2-cyclohexen-1-ol to form. The products from allylic oxidation is shown in Figure 4.26. The formation of the by-products is further confirmed in Figure 4.27.
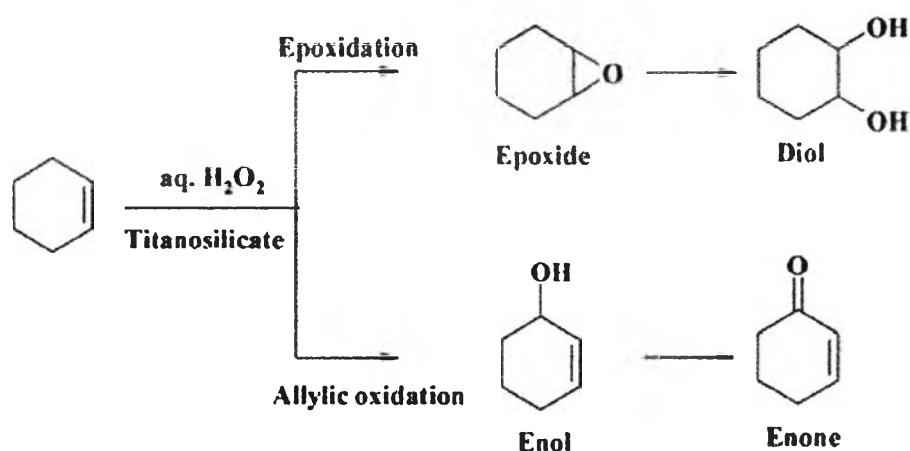
Figure 4.26 Side-products from allylic oxidation and ring opening.

(N. Bao *et al.*, 2010)
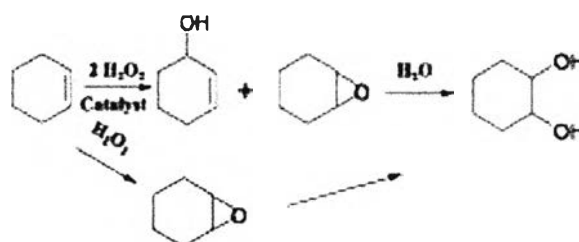
Figure 4.27 Side-products from cyclohexene epoxidation (A.S. Reddy *et al.*, 2010).

The reaction temperature was studied over the range of 50 – 90 °C. By increasing temperatures from 50 °C to 70 °C, the efficiency of the catalyst increases. The optimum yield of the products was gained at the temperature of 70 °C (24.6

%conversion; 69.6 %cyclohexene oxide selectivity; 17.1 %yield). After 70 °C, the efficiency of the catalyst to product cyclohexene oxide dropped drastically while there is an increase in the by-product's selectivity, especially *trans*-1,2-cyclohexanediol, increases. . The main cause should be the vaporization and decomposition of hydrogen peroxide (T. Sreethawong et al. 2006).

The catalyst amount was studied last, varying between 30 – 70 mg, shown in Figure 4.16 – 4.18. The trend of the graphs are similar to a mountain with the peak at 50 mg (28.8 %conversion; 68.4 %cyclohexene oxide selectivity; 19.71 %yield), indicating the optimum catalyst amount. More than 50 mg of the catalyst causes aggregation of the particles, limiting the accessibility of the reactants to the active sites, which in turn, lowers the conversion (T. Sreethawong et al. 2006).

In conclusion to all parameter investigation, the ideal conditions to use included 50 mg of 0.5%Ce/1%Ru/TiO$_2$ catalyst calcined at 500 °C for 4 hours at a ram rate of 1 °C, 30 mmol of cyclohexene, 30 ml of tert-butanol, and a reaction temperature of 70 °C. The reaction time used to compare all the results were done at the first hour.

4.2 N₂ Adsorption-Desorption Analysis

The surface area and porous qualities of a catalyst plays an inportant role as it is highly effective towards the reactivity and efficiency of the reaction. Monitoring the gas sorption on the surface of the catalyst enables calculatoin of these parameters. The amount of gas adsorbed on the monolayer determines the surface area while the porous qualities use calculation from the pore filling pressure.

All catalysts was put in the oven at 98 °C overnight prior to analysis.

The adsorption-desorption isotherms, Figure 4.28 – 4.31, of the TiO_2 (SG) , 1%Ru/TiO_2 (SSSG), 2%Ce/TiO_2 (SSSG) and 0.5%Ce/1%Ru/TiO_2 (SSSG) exhibit the IUPAC type IV pattern with hysteresis loop, implying the characteristic of mesoporous structure and narrow average pore size distribution. It is clearly observed that the sol-gel and single-step sol-gel synthesized catalysts exhibits higher surface area than the commercial TiO_2. Incorporating metals (Ce and Ru) lowers the mean mesoporous diameter while significantly increasing the total pore volume of the catalysts. The summary of all values are shown in table 4.3.
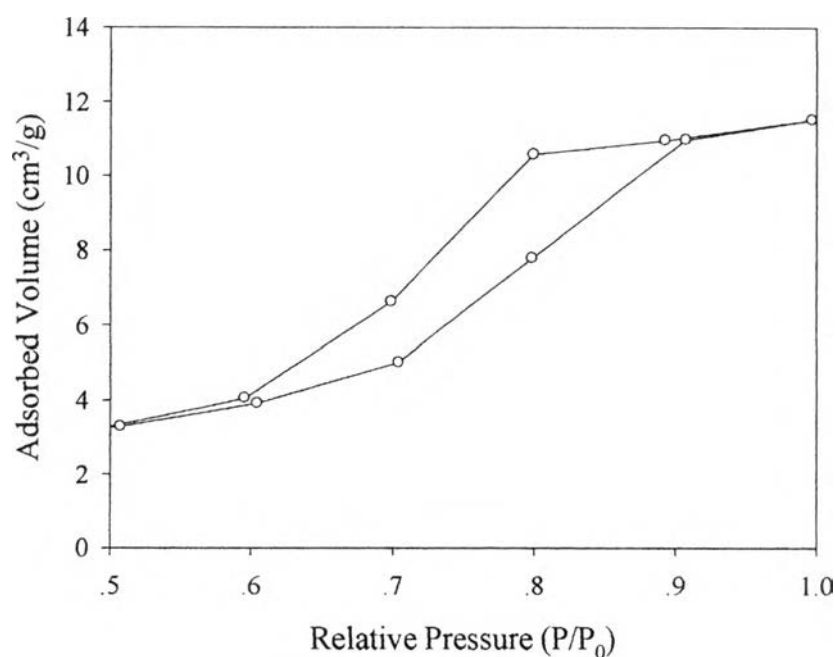
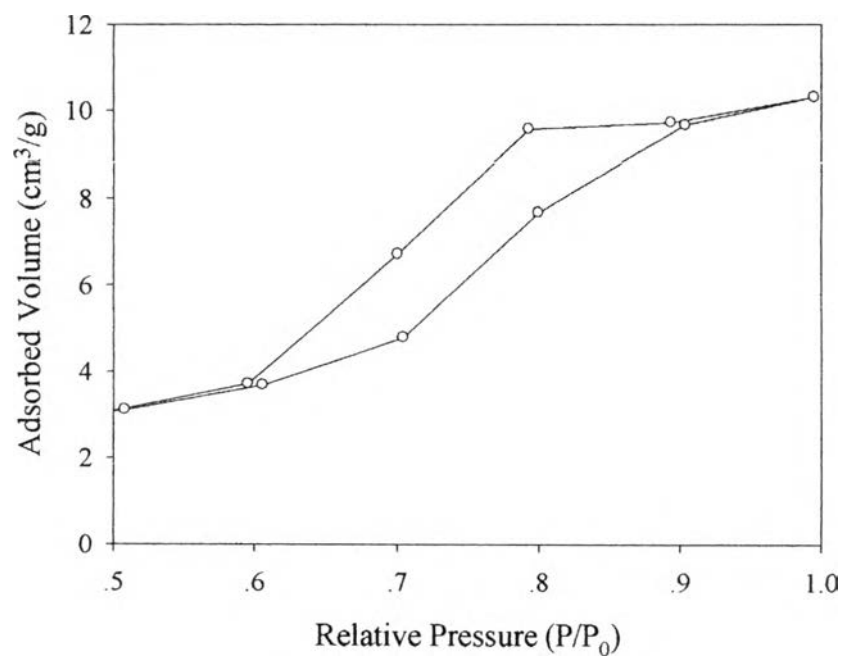**Figure 4.28** N₂ sorption isotherm of sol-gel TiO_2.
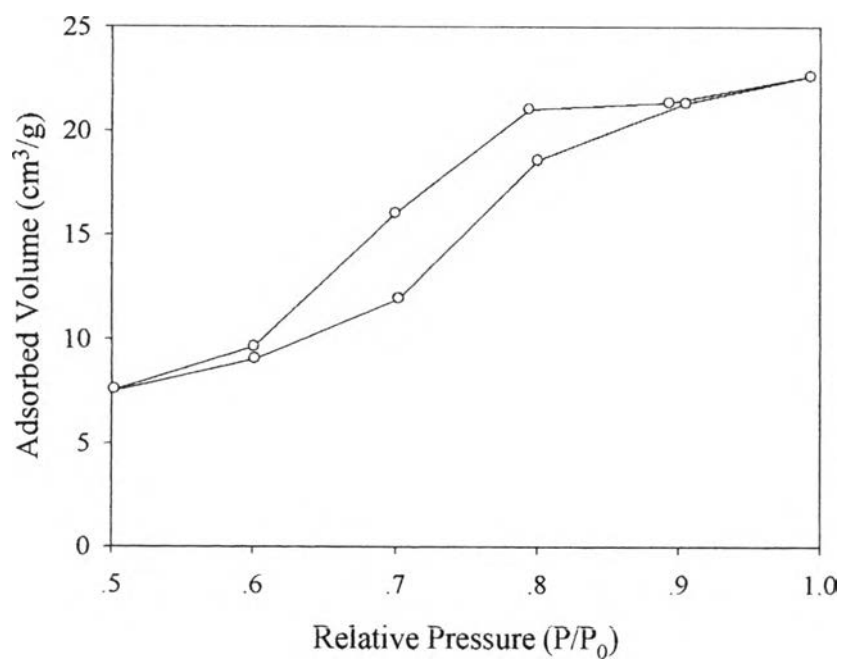
Figure 4.29 N_2 sorption isotherm of 1%Ru/TiO$_2$.

Figure 4.30 N_2 sorption isotherm of 2%Ce/TiO$_2$.
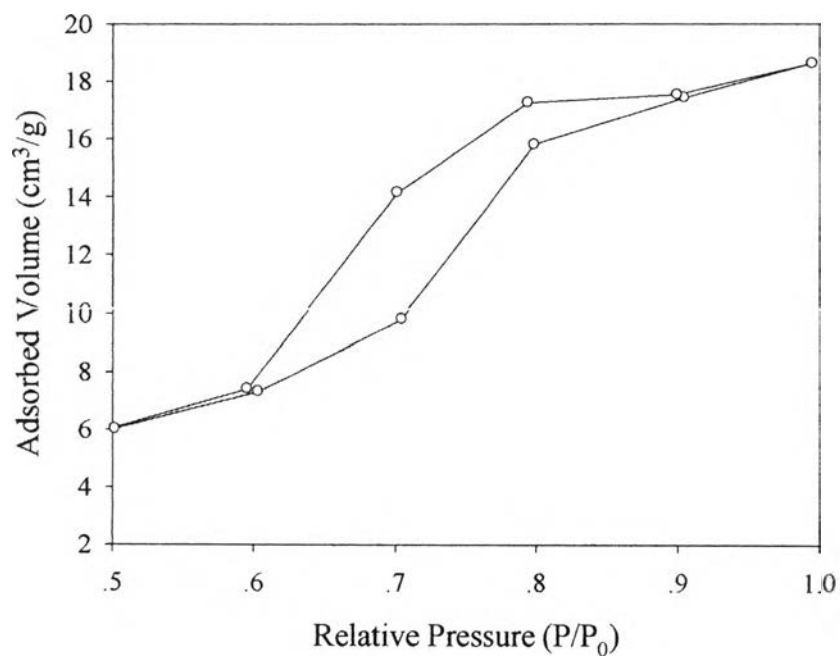
Figure 4.31 N_2 sorption isotherm of 0.5%Ce/1%Ru/TiO$_2$.

55

Table 4.3 Summary of BET results for TiO₂ (degussa P-25), sol-gel TiO₂ (reference), 1%Ru/TiO₂, 2%Ce/TiO₂, variation of Ce in the Ce/1%Ru/TiO₂ catalysts and variation of calcination conditions

Catalyst	Calcination temperature (°C)	Calcination time (h)	Calcination rate (°C/min)	BET	Mean mesopore diameter (nm)	Total pore volume (cm3/g)
P-25	-	-	-	59.2	-	-
TiO₂	500	4	10	68.9	8.1	0.12
1%Ru	500	4	10	72.9	6.11	0.17
2%Ce	500	4	10	129.9	6.16	0.26
0.5%Ce/1%Ru/TiO₂	475	4	10	122.9	6.13	0.25
	525	4	10	120.0	8.67	0.24
	500			102.6	6.14	0.24
	550			92.7	8.7	0.24
	500	1	10	129.2	6.14	0.26
		2		123.5	6.13	0.24
		3		120.1	6.13	0.25
		4		120.0	6.14	0.24
		5		107.5	8.73	0.25
	500	4	1	132.1	6.12	0.28
			5	128.7	6.16	0.25
			10	120.0	6.14	0.24
			15	115.7	6.13	0.24
1.0%Ce/1%Ru/TiO₂	500	4	10	119.8	6.14	0.26
1.5%Ce/1%Ru/TiO₂				138.5	6.16	0.3
2.0%Ce/1%Ru/TiO₂				139.4	6.15	0.28
2.5%Ce/1%Ru/TiO₂				137.4	6.16	0.3
3.0%Ce/1%Ru/TiO₂				139.2	6.17	0.31

The variations of ceria loading with TiO_2 support shows increase on all three properties with higher ceria metal amount. Higher porous diameters and porous volumes contribute to the higher surface area. Variation of calcination temperature shows decrease in BET surface area with higher temperatures. The increase of calcination temperature does not affect the total pore volume but increases the mean mesoporous diameter. Slower calcination ramp rates support higher surface area but are irrelevant to the mean diameter and total pore volume.

4.3 Thermogravimetric-Differential Thermal Analysis (TG-DTA)

The thermal gravimetric analysis (TGA) records the change in weight in relation to the increase in temperature. The TG/DTA curves of the uncalcined samples will be used to determine the appropriate calcination temperatures and their thermal decomposition. In addition, the method is also used in relation with the surface area analyzer to determine the surface hydroxyls.

Appropriate calcination temperatures are determined by the TG/DTA curves in Figures 4.32 for the uncalcined $0.5\%Ce/1\%Ru/TiO_2$. The weight loss from the DTG curve is approximately 43% for $0.5\%Ce/1\%Ru/TiO_2$.
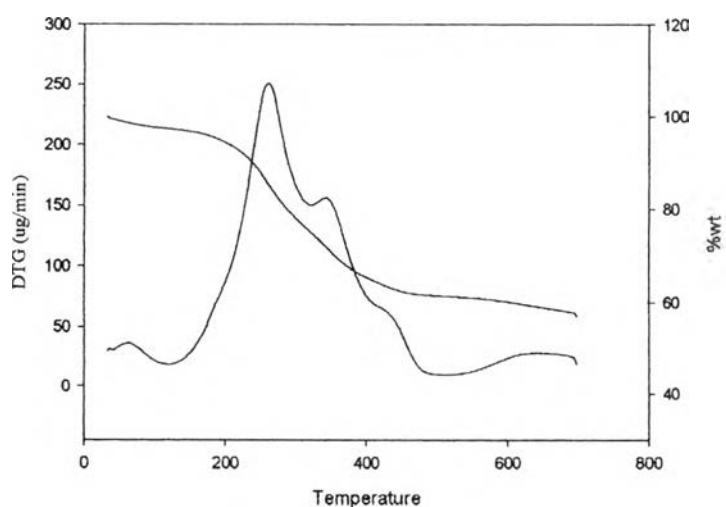
Figure 4.32 TG/DTA curve of the uncalcined 2%Ce on $1\%Ru/TiO_2$ support.

The uncalcined 0.5%Ce/1%Ru/TiO$_2$ shows three main exothermic peaks. The first peak, with temperatures less than 150 °C is contributed to the removal of water or moisture loosely bound to the surface of the catalyst. The second peak is between 150 °C to 350 °C which is achieved due to the removal of the organic surfactant template (LAHC) and the modifying agent (ACA). The last peak is between 350 °C to 500 °C. This peak represents the formation of the anatase phase in the structure as well as further removal of chemisorbed water and other organic remnants. It can be concluded that calcination at 500 °C is sufficient for the removal of moisture and remaining organics along with full formation of the anatase phase.

The surface of transitional metal oxides such as titania, ceria and ruthenium are mostly consists of hydroxyl groups. The hydroxyl groups on the surface of the catalyst will be determined. The OH surface density of the catalysts is calculated by using the TGA weight loss and the SAA, as shown in the equation below (Zou et al., 2004):

$$n\text{OH/nm}^2 = \alpha \left[\frac{(n\text{OH/nm}^2)_{T_2} \times \text{SSA} \times \text{wt}_{T_2} + \left(\dfrac{2(\text{wt}_{T_1} - \text{wt}_{T_2})N_A}{\text{MW}_{H_2O}} \right)}{\text{SSA} \times \text{wt}_{T_1}} \right]$$

(4.1)

where:

wt_{T_i}	= the sample weight at the corresponding temperature T_i
MW_{H_2O}	= the molecular weight of water (18 g/g-mol)
N_A	= Avogadro's constant (6.02×10^{23} mol^{-1})
SSA	= Specific surface area (m^2/g)
α	= a calibration factor given as 0.625
$(n\text{OH/nm}^2)_{T_2}$	= free of OH surface groups as 1 nm^{-2}
$n\text{OH/nm}^2$	= the OH surface density (nm^{-2})

Table 4.4 Summary of surface OH calculation results for sol-gel TiO_2 (reference), 1%Ru/TiO_2, 2%Ce/TiO_2, variation of Ce in the Ce/1%Ru/TiO_2 catalysts and variation of calcination conditions

Catalyst	Calcination temperature (°C)	Calcination time (h)	Calcination rate (°C/min)	BET	$W_{120°C}$	$W_{500°C}$	OH/nm^2
SG TiO_2	500	4	10	68.9	10.18	10.12	3.765
1%Ru	500	4	10	72.9	10.07	10.02	3.130
2%Ce	500	4	10	129.9	11.48	11.36	3.235
0.5%Ce/1%Ru/TiO_2	475	4	10	122.9	10.28	10.19	3.148
	500			120.0	10.34	10.25	3.164
	525			102.6	10.76	10.69	2.417
	550			92.7	9.94	9.88	2.755
	500	1	10	129.2	9.50	9.41	3.071
		2		123.5	10.25	10.16	3.065
		3		120.1	10.54	10.45	3.101
		4		120.0	10.34	10.25	3.164
		5		107.5	10.56	10.47	3.154
	500	4	1	132.1	10.26	10.13	3.982
			5	128.7	9.82	9.70	3.940
			10	120.0	10.34	10.25	3.164
			15	115.7	9.72	9.64	3.164
1.0%Ce/1%Ru/TiO_2	500	4	10	119.8	9.88	9.79	3.161
1.5%Ce/1%Ru/TiO_2				138.5	9.82	9.72	3.087
2.0%Ce/1%Ru/TiO_2				139.4	10.20	10.10	3.077
2.5%Ce/1%Ru/TiO_2				137.4	9.90	9.80	2.980
3.0%Ce/1%Ru/TiO_2				139.2	10.56	10.46	2.770

The highest surface hydroxyl was achieved when $0.5\%Ce/1\%Ru/TiO_2$ calcined at 500°C for 1 hours at a ramp rate of 1°C/min. The results correspond to the productivity of the catalyst characterized by the GC-FID.

4.4 X-ray Powder Diffraction (XRD) Analysis

Similar to a fingerprint, a unique diffraction pattern is obtained when X-Ray radiation interacts to each crystalline substance (phase). Therefore, the XRD is used for characterization and identification of polycrystalline phases. In addition, the integrated intensities of the peaks can be used to compare and relate the amount of each phase present in the sample. The crystallite size of the sample are calculated by utilizing the main characteristic peaks at $2\theta = 25.4°$ and $27.5°$, for anatase and rutile phase, respectively. The results from the crystallite size calculation are summarized in Table 4.5, at the end of this section.

XRD analysis was carried out using a Bruker AXS D8 Advance powder diffractometer with copper tube to emit $CuK\alpha$ radiation (1.5406 A°). The XRD generator voltage and current was 40 kV and 30 mA, respectively. The fixed goniometer parameters include 1° (2θ) divergent slit, 1° (2θ) scattering slit and 0.3 mm receiving slit. The analysis was performed over a scanning range of $2\theta = 20$-80°. The scan speed is 2° (2θ)/min with a scan step of 0.02° (2θ).

The phase behavior of sol-gel TiO_2, $1\%Ru/TiO_2$, $2\%Ce/TiO_2$ and $0.5\%Ce/1\%Ru/TiO_2$ are shown in Figure 4.33. Sol-gel TiO_2 shows diffraction peaks that represented the anatase phase ($2\theta = 25.4, 37.9, 48.1, 54.1$) while no indication of the brookite and rutile phase was present (L. Lopez et al., 2010).

Incorporation of $1\%Ru$ into the TiO_2 catalyst via single-step sol gel gives off a similar diffraction pattern as sol-gel TiO_2. The dominant peaks are of the anatase and rutile TiO_2, while two distinct peaks ($2\theta = 36.1, 41.3$) of RuO_2 can be seen, but with very low intensities. This can signify that the Ru is mostly in its amorphous state ($RuO_2 \cdot xH_2O$) and hardly changed into its crystalline form (W. Yong-gang, Z. Xiao-gang, 2004).

The sol-gel synthesized 2%Ce/TiO$_2$ catalyst shows diffraction patterns similar to that of sol-gel TiO$_2$ with high crystallinity. CeO$_2$ normally have indicative peaks as cubic fluorite CeO$_2$ (2θ = 28.57, 33.10, 47.53, 56.38) (S. Yang et al., 2006). Cubic CeO$_2$ are not present in the diffraction pattern due to the low amount of CeO$_2$ content in the sample. The higher amount of Ti phase encourages the dispersion of Ce in the Ti matrix, while lowering the chances of CeO$_2$ crystalline formation during calcination (M. Triki et al., 2009).

The diffraction pattern of the tri-metallic catalyst, 0.5%Ce/1%Ru/TiO$_2$, did not introduce any additional peaks from 1%Ru/TiO$_2$. The pattern is a combination of the peaks found in sol-gel TiO$_2$, 1%Ru/TiO$_2$, and 2%Ce/TiO$_2$. The results indicate that the interaction between the metals (Ce, Ru, and Ti) do not form new crystalline substances but are dispersed together in their respective crystalline forms (K.C. Fernandes et al., 2006).
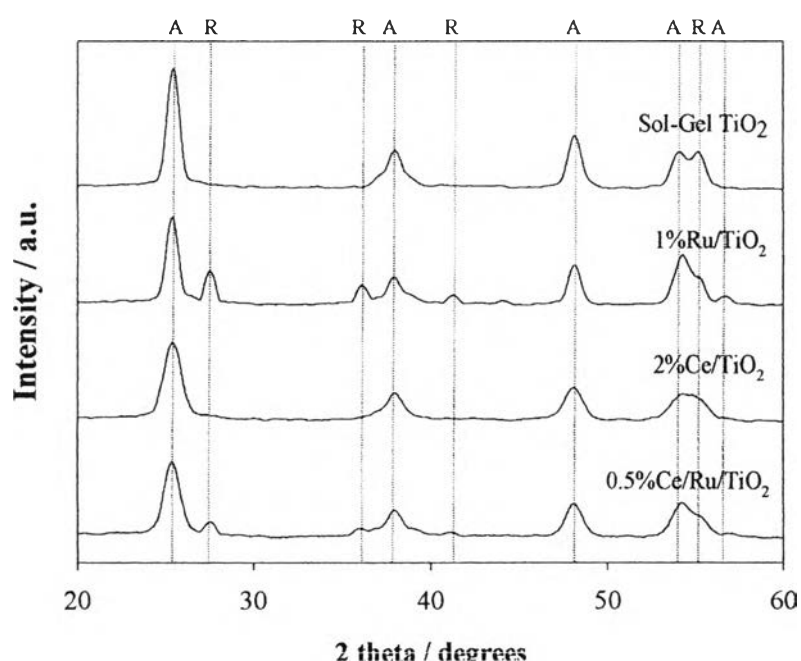

Figure 4.33 XRD patterns of sol-gel TiO$_2$, 1%Ru/TiO$_2$, 2%Ce/TiO$_2$ and 0.5%Ce/1%Ru/TiO$_2$. (Calcination conditions: temperature = 500 °C; ramp rate = 10 °C/min; time = 4 hours)

Many synthesis parameters were investigated in the experiments which affected the crystallinity of the catalyst. Diffraction patterns obtained from variation of Ce loading, calcination temperature, calcination time, and calcination ramp rate are depicted in Figure 4.34- 4.37, respectively.
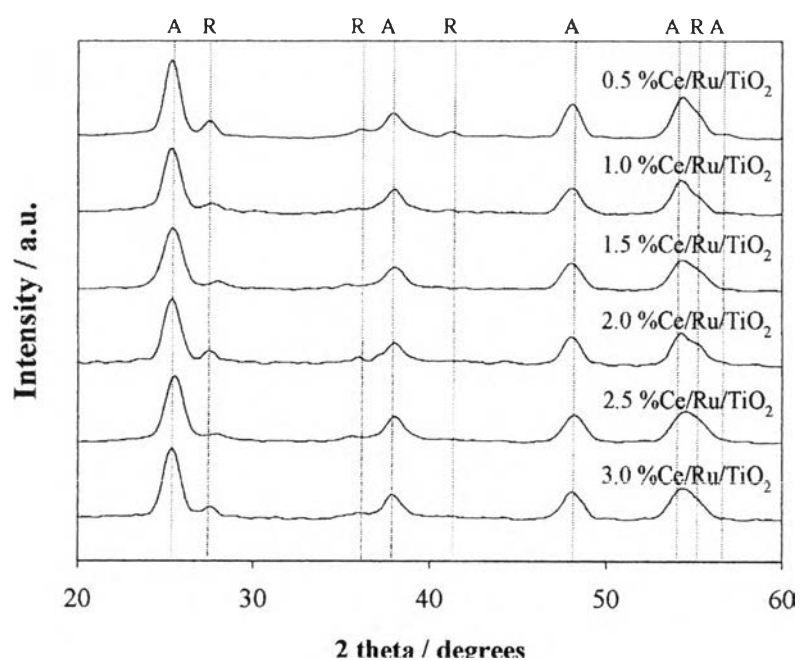
Figure 4.34 XRD patterns of Ce/1%Ru/TiO$_2$ calcined at 500 °C (ramp rate 10°C/min) for 4 hours with different Ce loadings: 0.5%, 1,0%, 1.5%, 2.0%, 2.5%, 3.0%.
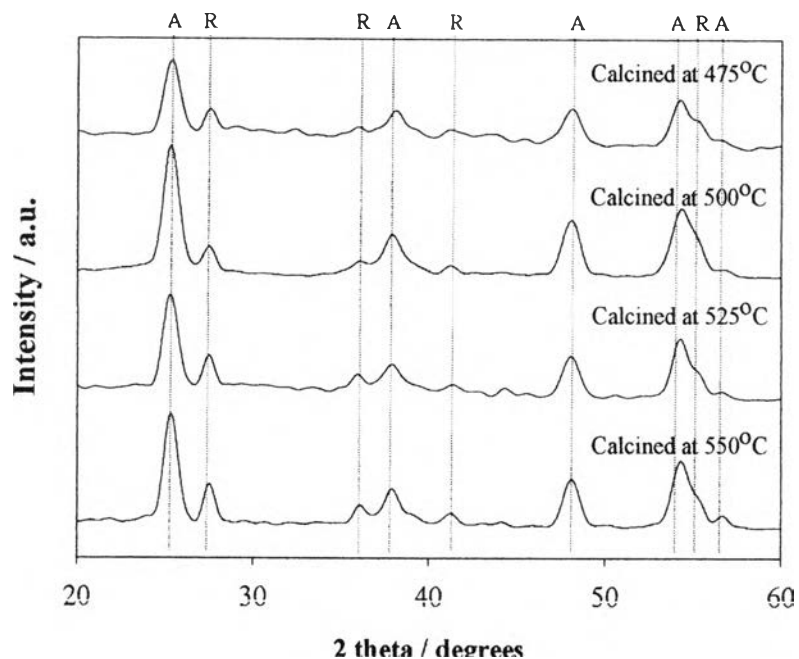
Figure 4.35 XRD patterns of 0.5%Ce/1%Ru/TiO$_2$ calcined for 4 hours (ramp rate 10 °C/min) with different calcination temperatures: 475 °C, 500 °C, 525 °C, and 550 °C.
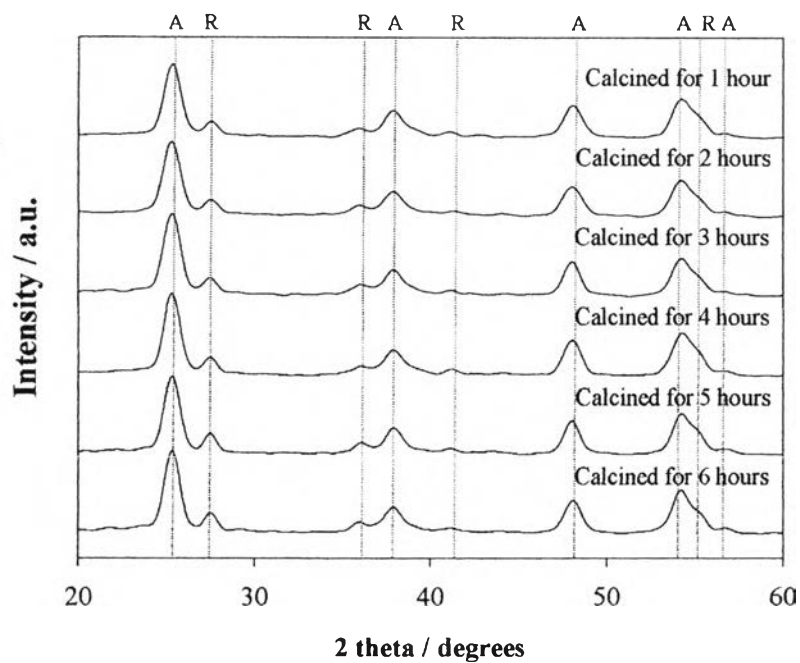
Figure 4.36 XRD patterns of 0.5%Ce/1%Ru/TiO$_2$ calcined at 500 °C with different calcination time: 1 hour, 2 hours, 3 hours, 4 hours, 5 hours, and 6 hours.
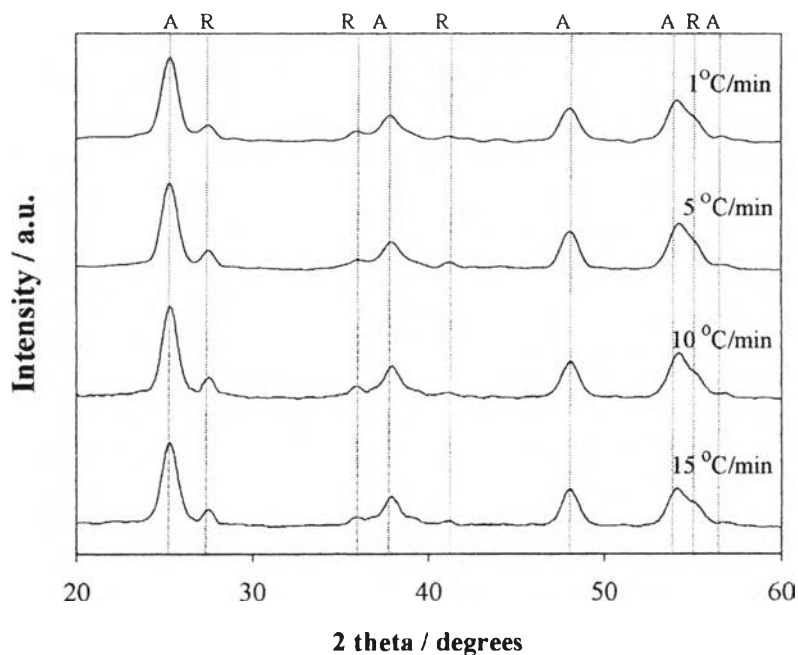
Figure 4.37 XRD patterns of 0.5%Ce/1%Ru/TiO₂ calcined at 500 °C for 4 hours with different calcination ramp rates: 1 °C/min, 5 °C/min, 10°C/min, and 15°C/min.

The variation of Ce content in this experiment was done between 0.5-3.0 mol%Ce in 1%Ru/TiO₂. Therefore, the catalysts are Ti-rich. The diffraction patterns coincide with that of 1%Ru/TiO₂. The increase in Ce content causes the peak to be slightly weaker and wider. This indicates that higher Ce contents lower the crystallite size of TiO₂. No crystalline phase attributed to CeO₂ was observed which is in agreement with the literature (B. Zhao et al., 2011) for Ti-rich Ce/TiO₂ catalysts. According to the literature, at higher Ce content (>20 %Ce), the peaks become visibly faint and asymmetric, signifying the oxides in amorphous state. As the Ce content becomes dominant (>50 %Ce), the only the cerianite CeO₂ peaks would be present, indicating solid solution formation with cerianite structure.

The anatase crystalline structure is dominant for the catalyst in the calcination temperature range of 475 – 550 °C. The increase in temperature leads nucleation of the rutile phase to slowly becoming the dominant peak, which is expected above 800°C (T. López et al., 2004). The literature suggests that the Ce

atoms are responsible for stabilizing the anatase TiO_2 phase, delaying crystallization into its rutile phase to higher temperatures.

The calcination time parameter had small effects on the crystallite size. However, calcination at 4 hours and ramp rate of 1°C/min gave the biggest crystallite size which is in agreement to the catalytic activity, having the highest yield.

Table 4.5 Summary of XRD analysis of the (A: Anatase, R: Rutile)

Catalyst	Calcination temperature (°C)	Calcination time (°C)	Calcination ramp rate (°C/min)	Phase from XRD Pattern	Crystallite size (nm) Anatase (101)	Rutile (110)
TiO$_2$	-	-	-	A	20.24	-
1%Ru	500	4	10	A+R	22.57	62.44
2%Ce	500	4	10	A	12.30	-
0.5%Ce/1%Ru/TiO$_2$	500	4	10	A+R	13.86	26.08
	525			A+R	13.86	26.08
	550			A+R	16.18	26.74
	500	1	10	A+R	12.99	23.18
		2		A+R	13.04	24.59
		3		A+R	14.23	26.36
		4		A+R	14.29	26.46
		5		A+R	14.21	25.62
		6		A+R	14.19	24.75
	500	4	1	A+R	13.48	30.10
			5	A+R	14.03	27.43
			15	A+R	15.56	26.12
1.0%Ce/1%Ru/TiO$_2$	500	4	10	A+R	13.15	26.21
1.5%Ce/1%Ru/TiO$_2$				A+R	13.10	25.98
2.0%Ce/1%Ru/TiO$_2$				A+R	12.32	25.57
2.5%Ce/1%Ru/TiO$_2$				A+R	12.23	17.92
3.0%Ce/1%Ru/TiO$_2$				A+R	12.19	12.27

## 4.5 Temperature Programmed Reduction (TPR) Analysis

The TPR analysis produces quantitative information on the reducibility of metal oxides. The results of the TPR profile for each type of catalyst are compared in Figure 4.38.

The TPR of sol-gel TiO_2 is considered asymmetric (S.A. da S. Corradini et al., 2008) to the axis as weak reduction peaks and hydrogen consumption can be seen approximately at 600 °C.

According to literature (S.A. da S. Corradini et al., 2008), the 1%Ru/TiO_2 catalyst typically shows a single reduction peak at 180 °C. The reduction is in agreement to the first peak found at 180 °C, attributed to the reduction of ruthenium oxide. The second peak is found at 230 °C, representing the reduction of large RuO_2 crystallites (A. Basińska et al., 2000). However, in addition to the two peaks, the catalyst shows another peak at 590 °C, which implies interaction between the RuO_2 and TiO_2.

CeO_2 is known to be reduced via a two-step mechanism. The first step is the reduction of the outer layer of Ce^{4+} at 400-550 °C, followed by reduction of the bulk at 750 °C (H.C. Yao et al., 1984). The TPR analysis shows 2%Ce/TiO_2 to have a very broad reduction band between 350-750 °C. Two main peaks are observed in the reduction at 400 °C and 700°C which represents the two steps of CeO_2 reduction.

The 0.5%Ce/1%Ru/TiO_2 shows overlapping peaks of 1%Ru/TiO_2 and 2%Ce/TiO_2. The two characteristic peaks of Ru are still apparent in the TPR profile with higher intensity. However, they slightly shifted to the left, resulted from the interaction between the Ce and Ru metals. The characteristic peaks of CeO_2 are barely noticeable. The typical bulk CeO_2 peak at 700 °C shifted to a lower temperature (600 °C), making a broad shoulder-like peak with the TiO_2 characteristic peak. It can be implied that the CeO_2 incorporated into the catalyst has become easier to reduce. Formation of CeO_2-TiO_2 solid solutions is also possible. A new identifiable peak is found at 320 °C. The peak is attributed to the interaction between Ce and Ru, also possibly forming a solid solution.
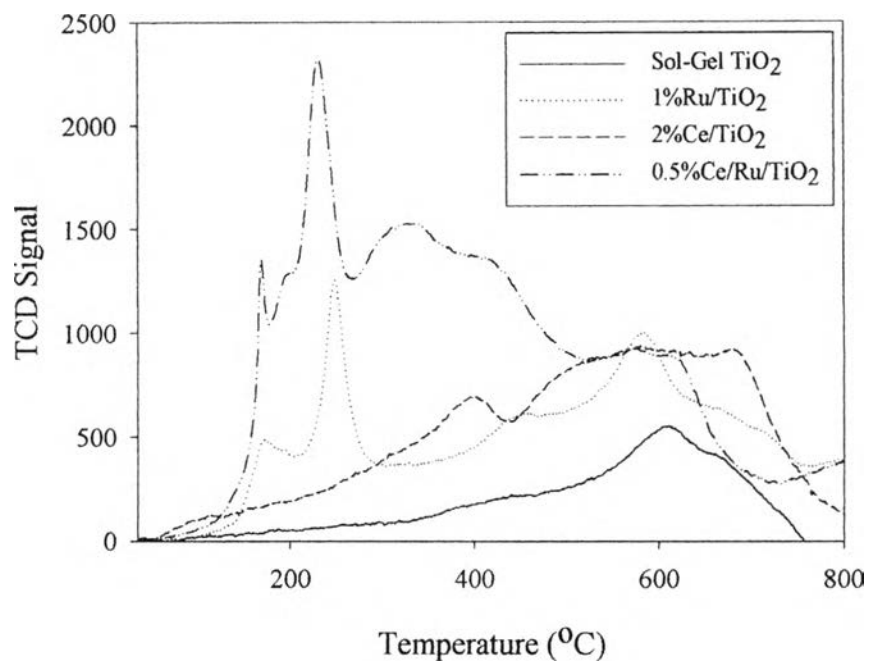
Figure 4.38 TPR profile of sol-gel TiO_2, 1%Ru/TiO_2, 2%Ce/TiO_2, and

0.5%Ce/1%Ru/TiO_2.